Conclusion: We have confirmed that the temperature-coefficient of the average dispersion of a ZDF transmission line is 100 times smaller than that of a conventional DSF. Temperature-independent 80Gbit/s OTDM transmission using the 168km ZDF transmission line has been successfully demonstrated. No penalty was observed for the ZDF transmission line over a temperature range of 50°C without adaptive dispersion equalisation while the penalty for 151km DSF transmission was 4.1dB.

Acknowledgment: The authors would like to thank M. Kawachi and K. Sato of NTT Network Innovation Laboratories and O. Mitomi of NTT Photonics Laboratories for their continuous encouragement.

10 December 1999

Electronics Letters Online No: 20000289

DOI: 10.1049/el:20000289

K. Yonenaga, A. Hirano, S. Kuwahara, Y. Miyamoto, H. Toba and K. Sato (*NTT Network Innovation Laboratories, 1-1 Hikarinooka, Yokosuka-shi, Kanagawa-ken, 239-0847, Japan*)

E-mail: yonenaga@exa.onlab.ntt.co.jp

H. Miyazawa (*NTT Photonics Laboratories, 3-1 Morinosato Wakamiya, Atsugi-shi, Kanagawa-ken, 243-0198, Japan*)

References

1 HAGIMOTO, K., YONEYAMA, M., SANO, A., HIRANO, A., KATAOKA, T., OTSUJI, T., SATO, K., and NOGUCHI, K.: 'Limitations and challenges of single-carrier full 40Gbit/s repeater system based on optical equalization and new circuit design'. Tech. Dig. OFC '97, Dallas, 1997, Paper ThC1, pp. 242–243

2 KIM, K.S., and LINES, M.E.: 'Temperature dependence of chromatic dispersion in dispersion-shifted fibers: Experiment and analysis', *J. Appl. Phys.*, 1993, **73**, (5), pp. 2069–2074

3 KUWAHARA, S., SANO, A., YONENAGA, K., MIYAMOTO, Y., and TOBA, H.: 'Simple zero dispersion detection technique using alternating chirp signal in automatic dispersion equalisation systems', *Electron. Lett.*, 1998, **34**, (20), pp. 1956–1958

4 SANO, A., KUWAHARA, S., and MIYAMOTO, Y.: 'Adaptive dispersion equalization of 8-ps pulses in 400-km transmission line by monitoring relative phase shift between spacing-fixed WDM signals'. Tech. Dig. OFC '99, San Diego, 1999, Paper WJ4, pp. 165–167

5 MUKASA, K., AKASAKA, Y., SUZUKI, Y., and KAMIYA, T.: 'Novel network fiber to manage dispersion at 1.55μm with combination of 1.3μm zero dispersion single mode fiber'. Tech. Dig. ECOC '97, Edinburgh, 1997, Vol. 1, pp. 127–130

6 MIYAMOTO, Y., YONENAGA, K., HIRANO, A., SHIMIZU, N., YONEYAMA, M., KATARA, H., NOGUCHI, K., and TSUZUKI, K.: '1.04-Tbit/s DWDM transmission experiment based on alternate-polarization 80-Gbit/s OTDM signals'. Tech. Dig. ECOC '98, Madrid, 1998, Post-Deadline Papers, pp. 53–57

7 YONENAGA, K., and MIYAMOTO, Y.: 'Dispersion-managed high-capacity WDM systems using zero-dispersion-flattened transmission line', Paper FD4, Tech. Dig. OFC '99, 1999, (San Diego),pp. 71–73

8 OTSUJI, T., YONEYAMA, M., IMAI, Y., ENOKI, T., and UMEDA, Y.: '64 Gbit/s 2:1 multiplexer IC using InAlAs/InGaAs/InP HEMTs', *Electron. Lett.*, 1997, **33**, (17), pp. 1488–1489

9 NOGUCHI, K., MITOMI, O., and MIYAZAWA, H.: 'Low-voltage and broadband Ti:$LiNbO_3$ modulators operating in the millimeter wavelength region'. Tech. Dig. OFC '96, San Jose, 1996, Paper ThB2, pp. 205–206

10 SATO, K., HIRANO, A., ASOBE, M., and ISHII, H.: 'Chirp-compensated 40 GHz semiconductor modelocked lasers integrated with chirped grating', *Electron. Lett.*, 1998, **34**, (20), pp. 1944–1946

Wavelength routing of 40Gbit/s packets with 2.5Gbit/s header erasure/rewriting using all-fibre wavelength converter

B.-E. Olsson, P. Öhlén, L. Rau, G. Rossi, O. Jerphagnon, R. Doshi, D.S. Humphries, D.J. Blumenthal, V. Kaman and J.E. Bowers

40Gbit/s packet wavelength routing and 2.5Gbit/s header replacement is demonstrated using an ultra-high-speed wavelength converter. Burst-mode bit error rate measurements are performed on both the header and payload before and after wavelength routing, with < 4dB penalty in the payload and < 2.5dB penalty in the header.

Introduction: The exponential growth in Internet traffic is forcing next generation IP data networks to a scale far beyond present performances. Optical packet switching technologies may be required to deliver low-latency packet forwarding and routing at terabit wire rates and should support header erasure and rewriting. The latter is important for all-optical label swapping (AOLS) [1] and new simpler IP routing protocols such as multi-protocol label switching (MPLS) [2]. Initial experiments on AOLS with packet rate wavelength conversion [3] and optical packet switching [4] have been reported as well as basic routing experiments at 100Gbit/s using all-optical header processing [5]. However, demonstrations of wavelength routing with bit error rate (BER) measurements and header replacement have been limited to bit rates at 10 Gbit/s or below, mainly due to speed limitations in the wavelength converter technology. In this Letter we report the wavelength routing of packets with 40Gbit/s return-to-zero (RZ) payloads and replacement of 2.5 Gbit/s time domain non-return-to-zero (NRZ) headers. Every other packet is routed to two different wavelengths while simultaneously erasing the old header and rewriting a new one on the new wavelength. A novel wavelength converter (WC) [6] plays a key role in the header replacement process by wavelength converting the payload while simultaneously erasing and rewriting the header. Burst-mode BER measurements were performed on packets for the payload before and after wavelength conversion, and on the original and the replaced header. The possible switching speed and packet length in this architecture are determined by the tunable laser in the wavelength converter, presently ~5ns. The WC is based on cross-phase modulation (XPM) in an optical fibre, which has the potential for operating at ultra-high bit rates. When the incoming data are combined with a continuous wave (CW) signal and sent through an optical fibre, the data impose a phase modulation on the CW light through XPM. This phase modulation generates optical sidebands in the CW signal, which can be converted to amplitude modulation by suppressing the original CW carrier using an optical notch filter. In this Letter, a loop mirror filter (LMF) was used which consisted of a short piece of birefringent fibre in a Sagnac interferometer. Such a filter is tunable, polarisation independent, and has repetitive notches, which enables conversion to different equally spaced wavelengths to be achieved without any further adjustment. The transfer function of the WC is nonlinear, thus if the amplitude of the input signal is low, a very small portion is converted to the new wavelength. This phenomenon is used to remove the header of the packet since the header peak power can be substantially lower than the RZ payload while still keeping the same energy per bit in the header and the payload.

Experimental results: Fig. 1 shows the experimental setup. The packet generator consisted of an actively modelocked fibre ring laser generating 10ps pulses with a time-bandwidth product (TBP) of 0.45 at 1536nm followed by an $LiNbO_3$ modulator encoding 10Gbit/s PRBS data with a word length of 2^{31}–1. The 10Gbit/s data were injected into a passive 10 to 40Gbit/s multiplexer consisting of polarisation maintaining (PM) fibre with 75 and 150ps delays. An acousto-optical modulator (AOM) gated out a 2.5μs payload that was combined with a 2.5Gbit/s (PRBS 27–1) 500ns long header. The header was aligned in front of the payload with a 100ns guard band determined by the 100ns rise time in the AOM, and a 100ns guard band was inserted between each packet, giving a total packet length of 3.2μs. The packets were injected into the WC which consisted of an erbium-doped fibre amplifier

(EDFA) with an average output power of +18dBm followed by 5km dispersion-shifted fibre (DSF) with a zero-dispersion wavelength of 1542nm. A grating coupled sampled rear reflector (GCSR) laser [7] that could be tuned to either 1538 or 1543nm within 5ns determined the new wavelength. The GCSR laser was also used to encode the new 2.5Gbit/s header before entering the WC. After the DSF, an LMF, consisting of a loop mirror with 4m of PM fibre and a polarisation controller to allow adjustment of the filter wavelength, was used to suppress the original CW light. The separation between the notches was 1 nm (given by the length of the PM fibre) and the suppression was better than 27dB. A second filter was used to select one of the two sidebands and to suppress the original data. The use of only one sideband retained the pulse width and TBP from the input pulse. The 40Gbit/s receiver consisted of a 40 to 10Gbit/s demultiplexer followed by a 10Gbit/s preamplified receiver. The demultiplexer was based on an electroabsorption modulator (EAM), driven with a 30ps electrical pulse to achieve a 15ps switching window. The 2.5Gbit/s header receiver consisted of an AOM to remove the payload, which otherwise would dominate the measured optical average power, followed by an optically preamplified receiver. The BER measurements were made on both the payload and header, and gated to select the appropriate time interval.

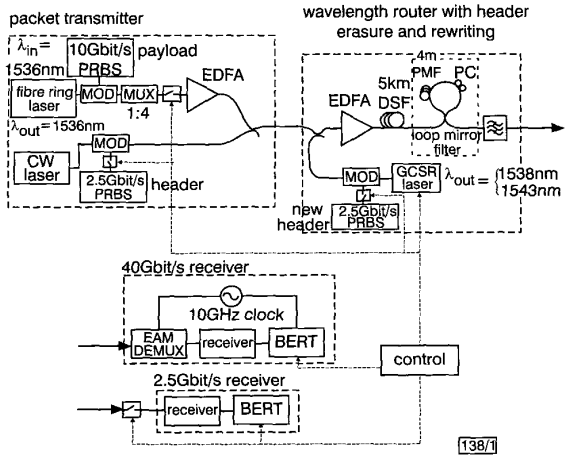

Fig. 1 *Experimental setup*

MOD: $LiNbO_3$ modulator; MUX: passive 10 to 40 Gbit/s multiplexer; PC: polarisation controller; EAM DEMUX: demultiplexer using electroabsorption modulator; BERT: bit error rate test set

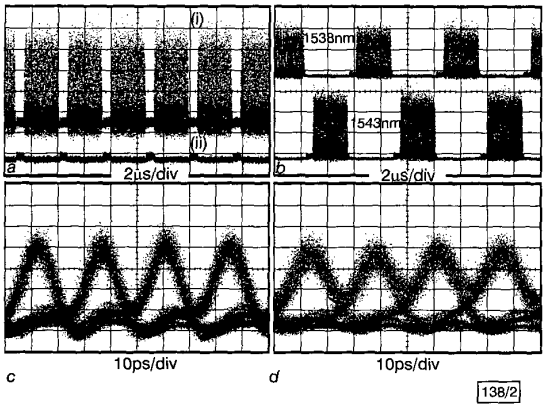

Fig. 2 *Packets and eye-patterns before and after wavelength routing*

a Packets before wavelength routing
(i) 40Gbit/s RZ payload and 2.5Gbit/s NRZ header
(ii) headers without payload
b 40Gbit/s eye-patterns before wavelength routing
c Packets routed to 1538 and 1543nm
d Eye pattern of routed packet at 1543nm

Fig. 2*a* shows the input packets consisting of the 40Gbit/s RZ payload and the 2.5Gbit/s NRZ header with ~10dB less peak power. The lower trace shows the headers without the payload. Fig. 2*b* shows every other packet routed to 1538 and 1543nm with new inserted headers. The eye patterns of Fig. 2*c* and *d* were taken zooming into the payload, before (1536nm) and after the WC (1543nm). BER measurements were performed on both the header and payload on incoming and outgoing packets. The BER detector was gated and error measurements could only be performed on ~80% of all bits in the packets due to the number of bits required to synchronise the BER detector. Fig. 3*a* shows the BER for all four 10Gbit/s TDM channels in the 40Gbit/s payload for the input packets at 1536 nm and the output packets at 1543 and 1538nm. All channels at both output wavelengths have < 4dB penalty compared with the input packets, and this penalty is believed to be due to non-optimal filtering in the wavelength converter and to polarisation instabilities in the input 40Gbit/s data.

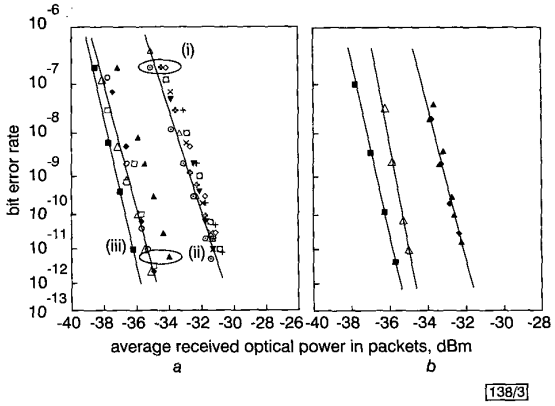

Fig. 3 *Bit error rate measurements*

a Bit error rate measurements for 40Gbit/s before and after wavelength routing
■ 10Gbit/s data
△ 10Gbit/s packet
▲ channel 1, 1536nm
◆ channel 2, 1536nm
□ channel 3, 1536nm
○ channel 4, 1536nm
△ channel 1, 1538nm
◇ channel 2, 1538nm
▼ channel 3, 1538nm
× channel 4, 1538nm
⊙ channel 1, 1543nm
⊕ channel 2, 1543nm
⊡ channel 3, 1543nm
+ channel 4, 1543nm
(i) 40Gbit/s wavelength conversion
(ii) 40Gbit/s input packets
(iii) 10Gbit/s baseline
b Bit error rate measurements for 2.5Gbit/s baseline, original header and replaced headers
■ baseline CW
△ original header
▲ header 1538nm
◆ header 1543nm

At 10Gbit/s wavelength conversion the penalty was < 1dB which indicates that a major part of the penalty is due to instabilities in the 40Gbit/s data. Fig. 3*b* shows BER measurements of the old and replaced headers. The old header is completely removed in the wavelength converter and a new header could be successfully inserted, with no crosstalk penalty from the old header. However, a receiver penalty of 2.5dB was measured, probably due to distortion from the sharp notches of the LMF. In a filter with a flatter stop band, e.g. a fibre Bragg grating, this distortion would probably be avoided.

Acknowledgment: This work was supported under the DARPA sponsored MOST center (F49620-96-1-0349) and DARPA NGI grant (MDA972-99-1-0006).

27 December 1999
Electronics Letters Online No: 20000235
DOI: 10.1049/el:20000235

B.-E. Olsson, P. Öhlén, L. Rau, G. Rossi, O. Jerphagnon, R. Doshi, D.S. Humphries and D.J. Blumenthal (*Optical Communications and Photonic Networks Group, University of California, Department of Electrical and Computer Engineering, Santa Barbara, CA 93106, USA*)

V. Kaman and J.E. Bowers (*Ultrafast Optoelectronics Research Group, University of California, Department of Electrical and Computer Engineering, Santa Barbara, CA 93106, USA*)

P. Öhlén: On leave from Royal Institute of Technology, Sweden

G. Rossi: On leave from University of Pavia, Italy

References

1 BLUMENTHAL, D.J., *et al.*: 'All-optical label swapping with wavelength conversion for WDM-IP networks with subcarrier multiplexed addressing', *IEEE Photonics Technol. Lett.*, 2000, **11**, pp. 1497–1499

2 VISWANATHAN, A., *et al.*: 'Evolution of multiprotocol label switching', *IEEE Commun. Mag.*, 1998, **36**, pp. 165–173

3 CARENA, A., *et al.*: 'OPERA: An optical packet experimental routing architecture with label swapping capability', *J. Lightwave. Technol.*, 1998, **LT-16**, pp. 2135–2145

4 CHIARONI, D., *et al.*: 'Physical and logical validation of a network based on all-optical packet switching systems', *J. Lightwave. Technol.*, 1998, **LT-16**, pp. 2255–2264

5 TOLIVER, P., *et al.*: 'Routing of 100Gb/s word in a pocket-switched optical networking demonstration (POND) node', *J. Lightwave. Technol.*, 1998, **LT-16**, pp. 2169–2180

6 OLLSON, B.E., *et al.*: 'A simple and robust high-speed wavelength converter using fiber cross-phase modulation and filtering'. Proc. Opt. Fiber Comm. Conf., 2000, Baltimore, USA, Paper WE1

7 RIGOLE, P.-J., *et al.*: '114-nm wavelength tuning range of a vertical grating assisted codirectional coupler laser with a super structure grating distributed Bragg reflector', *IEEE Photonics Technol. Lett.*, 1995, **7**, pp. 697–699

Characterisation of single stage, dual-pumped Raman fibre amplifiers for different gain fibre lengths

F. Koch, S.V. Chernikov, S.A.E. Lewis and J.R. Taylor

The power dependent gain length of dispersion shifted fibre Raman amplifiers has been characterised. The noise performance has also been investigated.

Broadband silica fibre Raman amplifiers (FRAs) are particularly attractive for ultra-broadband applications in telecommunications. Raman amplifiers can operate throughout the low loss window of optical fibres from 1.1 to 1.7μm compared with conventional erbium doped amplifiers which are deployed in the 1.55μm region. Raman amplification offers the advantages of greatly extended bandwidth and distributed amplification [1] with the installed fibre as the gain medium. Here we report the characterisation of the pump power requirements and spontaneous noise performance of a dual wavelength pumped Raman amplifier for a wide range of gain fibre lengths covering the range applicable to discrete or distributed amplification.

The amplifier was constructed from sections of dispersion shifted fibre of different lengths spliced together, with optical circulators employed to multiplex and demultiplex the pump and signal. The single stage amplifier was counter-pumped [2] using fibre Raman lasers operating at fundamental wavelengths of 1423 and 1455nm. This configuration allows broadband amplification in the 1.5μm region [3, 4]. For each amplifier length, the pump power was adjusted to achieve a peak gain of 15dB. At lower pump power levels the trends shown in the gain and noise figures were similar to those at 15 dB which are exclusively reported in this Letter.

A CW diode laser tunable from 1500 to 1580nm at a power of -20dBm was used as the signal source. The measurements were carried out with a computer-automated system controlling the tunable laser and optical spectrum analyser using the spectral division method. For each amplifier length the pump power was adjusted to equalise the gain peaks to 15dB. The pump power was calibrated using a broadband thermal detector with an accuracy of 6%, with the error in this measurement arising primarily from the calibration of the power meter and an additional small systematic error dependent on the repeatability of the splice to the circulator. Unlike the erbium amplifier the spontaneous noise figure does not depend sensitively on the pump power.

Fig. 1 shows the required pump powers for the 1423 and 1455nm pumps to achieve a 15dB gain at the two gain peaks around 1523 and 1555nm, respectively. The short wavelength pump is operated at a higher power due to the inter-pump Raman interaction which causes a progressive power transfer from the short to the long wavelength pump as these signals propagate along the length of the amplifier. The overall required pump power decreases with the amplifier length as the effective nonlinear interaction length grows, while the differential pump power increases as a result of the inter-pump interaction. Around an amplifier length of ~23km the amplifier starts to become very weakly pumped at the input and the pump power at 1423nm has to be increased to maintain the desired gain. In the case of an unsaturated amplifier the maximum gain is limited by the direct loss at the signal wavelength and the effective length given by the loss at the pump wavelength [5]. From the minimum required pump power from Fig. 1 it can be estimated that the pump power is used most efficiently for the 1423nm pump when the amplifier length is less than ~23km. This length is slightly longer than the effective nonlinear length for a single wavelength pumped amplifier as a result of the inter-pump Raman interaction.

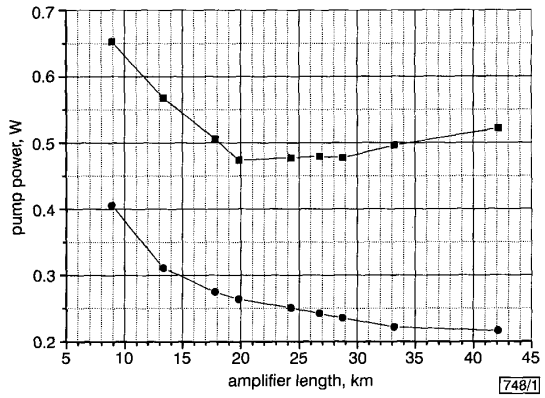

Fig. 1 *Required pump power for 15dB maximum gain*
■ 1423nm
● 1455nm

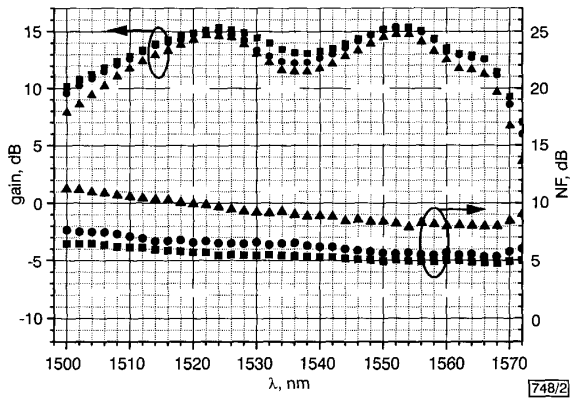

Fig. 2 *Noise figure and gain for different amplifier lengths*
■ 9km
● 19km
▲ 46km

Fig. 2 shows the representative gain and noise figure spectra for three different lengths for peak gains of 15dB. All the measurements include the loss of the splices and circulator coupling losses which add to the noise figure. The variations in the gain shape are mainly due to slight variations in the pump peak wavelength and spectral width with different pump powers. Some gain narrowing occurs for longer fibre lengths because the gross gain is higher to compensate for the increased loss, but the main contribution is due to the pump variations. This has been confirmed by numerical simulation [3]. The variation in noise figure for three representative wavelengths is shown against amplifier length in Fig. 3. As expected, the noise figure increases with length as the fibre becomes less strongly pumped at the amplifier input and, for